The CLAMP GA-binding transcription factor regulates heat stress-induced transcriptional repression by associating with 3D loop anchors

Joseph Aguilera[1], Jingyue Duan[2], So-min Lee[1], Mukulika Ray[1*] and Erica Larschan[1*]

*Co-corresponding authors

[1] MCB department, Brown University, Providence, RI, USA
[1] Cornell Animal Science, College of Agriculture and Life Sciences, Cornell University, Ithaca, NY, USA

Abstract

In order to survive when exposed to heat stress (HS), organisms activate stress response genes and repress constitutive gene expression to prevent the accumulation of potentially toxic RNA and protein products. Although many studies have elucidated the mechanisms that drive HS-induced activation of stress response genes across species, little is known about repression mechanisms or how genes are targeted for activation versus repression context-specifically. The mechanisms of heat stress-regulated activation have been well-studied in *Drosophila,* in which the GA-binding transcription factor GAF is important for activating genes upon heat stress. Here, we show that a functionally distinct GA-binding transcription factor (TF) protein, CLAMP (Chromatin-linked adaptor for MSL complex proteins), is essential for repressing constitutive genes upon heat stress but not activation of the canonical heat stress pathway. HS induces loss of CLAMP-associated 3D chromatin loop anchors associated with different combinations of GA-binding TFs prior to HS if a gene becomes repressed versus activated. Overall, we demonstrate that CLAMP promotes repression of constitutive genes upon HS, and repression and activation are associated with the loss of CLAMP-associated 3D chromatin loops bound by different combinations of GA-binding TFs.

Introduction

Understanding how external stimuli regulate gene expression is essential for reducing the effects of dynamic changes in abiotic factors on all living organisms. One such external stimulus, temperature, plays a vital role in determining viability and fertility, which often decrease as temperatures rise (1). Heat stress (HS) rapidly changes transcription of both heat stress genes which become activated and constitutive genes which become repressed (2,3). Therefore, understanding the mechanisms that drive changes in transcription upon heat stress will provide critical insight into how transcription rapidly alters in response to stimuli. Because the heat stress response is rapidly inducible, many discoveries of fundamental transcriptional mechanisms have been made using this system, including pausing of RNA Polymerase II, which occurs at thousands of genes across species (4).

Heat stress induces two types of transcriptional changes: 1) activation of heat shock-induced genes; 2) repression of constitutively active genes (5). Best studied in *Drosophila*, decades of research have defined mechanisms of heat stress-induced gene activation at heat shock responsive genes whose promoters have specific DNA sequences called **H**eat **s**hock responsive **e**lements (HSEs), bound by Heat Shock Factor (HSF) (4,6,7). In *Drosophila*, the GA-binding transcription factor GAF and transcription elongation factor NELF, which regulates RNA Polymerase II pause release, are also involved in heat stress-regulated gene activation (7-9). Furthermore, in mammals, NELF has roles in activation and repression mediated by phase transition caused by HS (10). However, it is not known what drives the context-specific function of NELF as an activator or a repressor at specific target genes.

In contrast to activation, much less is known about the specific DNA binding factors that target constitutive genes for repression after heat stress. Transcriptional repression involves a decrease in promoter-proximally paused RNA Polymerase II at repressed genes (3,7) and cryptic premature termination of transcripts with impaired elongation rate and decreased processivity (10,11). A report also suggests that heat stress induces the relocalization of architectural proteins from TAD borders to Polycomb binding sites at the interior of TADs, which changes 3D chromatin architecture and may regulate repression (12). However, the role of 3D chromatin architectural

changes during the heat stress response still needs to be better understood because another report suggests that global 3D architectural changes at the TAD and compartment level do not occur upon HS but did not examine chromatin loops (2). Therefore, the mechanisms by which 3D chromatin changes regulate the heat stress response requires further study.

Furthermore, HSF and GAF are involved in heat-stress-induced activation but not heat-stress-induced repression. GAF has context-dependent synergistic or antagonistic relationships with another GA-binding transcription factor, CLAMP (Chromatin-linked adaptor for MSL complex proteins)(13,14). Although these two transcription factors have similar DNA recognition sequences, variation within seemingly similar *cis*-elements drive the context-specific targeting of CLAMP to the male X-chromosome and the histone locus, where it inhibits GAF binding (13,15). Also, CLAMP promotes long-range 3D chromatin interactions (16) and interacts with NELF, which functions in heat shock activation and repression (10,17). Therefore, we hypothesized that CLAMP regulates heat stress-dependent transcription.

To test our hypothesis, we used two approaches: 1) nascent RNA-sequencing (SLAM-seq) to identify the function of CLAMP in heat stress-induced gene activation and repression; 2) HiChIP to identify CLAMP-associated 3D chromatin loop anchors associated with heat-stress-dependent transcriptional regulation. We found that, unlike GAF, CLAMP regulates heat-stress-induced transcriptional repression at many more genes than activation. Furthermore, CLAMP-dependent repression of genes upon heat stress is strongly associated with loss of CLAMP-bound 3D chromatin loop anchors but not changes in CLAMP occupancy on chromatin. In addition, prior to heat stress, different GA-binding factors interact with CLAMP-bound loop anchors near genes that will become repressed compared with genes that will become activated upon heat stress. Therefore, the combination of GA-binding factors that interact with a gene may promote context-specific repression versus activation of target genes after heat stress.

Results

1. CLAMP is required for the repression of transcription after heat stress

To understand how the CLAMP GA-binding TF regulates transcription after heat stress, we performed high-throughput sequencing of nascent RNA in *Drosophila* Kc cells using Thiol(SH)–linked alkylation for the metabolic sequencing of RNA (SLAM-seq)(18). SLAM-seq quantifies nascent mRNA by measuring 4SU (4-thiouridine) incorporation as thymine-to-cytosine (T to C) conversions. Cells were incubated in 4SU either at RT for one hour (No heat stress, NHS) or at 37∘C for one hour (Heat stress, HS) and immediately processed to identify which mRNAs incorporated 4SU within the total mRNA pool. Next, we compared the mRNAs incorporating 4SU under HS and NHS conditions and determined which transcripts were increased after heat stress (activated genes) and which transcripts were reduced (repressed genes) during HS (FDR cutoff of $p \geq 0.05$ and $\log2FC \geq 2$).

Consistent with a prior report (7), we identified a subset of transcripts activated (**N=995**) and a more extensive set repressed (**N=3547**) in control *gfpRNAi*-treated cells after HS (**Figure 1A**). Activated transcripts include all the known heat shock-responsive genes, including the transcripts for heat shock chaperone proteins (**Table 1a**). Much less is known about the mechanisms mediating heat-stress-induced repression than activation. We hypothesized that repression is mediated by the CLAMP GA-binding protein TF because it is known to compete with GAF, which regulates heat-stress-induced activation (7,13). Because CLAMP regulates dosage compensation in addition to global transcription in males, we examined the function of CLAMP in regulating the heat stress response in Kc cells, which are female.

In the absence of heat stress (NHS), our validated *clamp* RNAi treatment (13,19,20) causes increased levels of 987 nascent transcripts and decreased levels of 246 nascent transcripts. Therefore, CLAMP functions as a repressor more frequently than an activator in Kc cells prior to heat stress (**Fig S1A, Table 1b**). After HS, we observed an even more substantial widespread increase in transcript levels in *clamp* RNAi-treated cells compared with control *gfp* RNAi-treated cells (4028 upregulated transcripts; 58 downregulated transcripts) (**Figure 1B, Fig S1B, Table**

1c). To determine how CLAMP regulates genes that are typically repressed upon heat stress, we measured the percentage of genes that are usually repressed in *gfp* RNAi-treated cells that remain repressed in *clamp* RNAi-treated cells and found that only 4.4% **(155/3547)** of transcripts remain repressed after *clamp* RNAi. (**Figure 1A**). Therefore, CLAMP promotes transcriptional repression of 95.6% of constitutive genes after heat stress.

In order to test whether CLAMP promotes repression of heat stress response genes in the fly, we examined the distribution of active RNA Polymerase II on polytene chromosomes after HS (37°C) in control (undriven *clamp RNAi*) and *fkh-GAL4>clampRNAi* larvae (**Figure 1C**). Consistent with extensive prior work (21,22), heat stress restricts the binding of active RNA polymerase II (red) to specific cytological positions corresponding to heat stress responsive loci (**Figure 1C**). In contrast, after *clamp* RNAi, active RNA Polymerase II (red) remains bound genome-wide, including at essential heat stress responsive loci, suggesting a loss of repression but not activation. In flies, CLAMP is retained after *clamp* RNAi treatment only at the histone locus, perhaps because it contains 200 CLAMP binding sites (15). Therefore, CLAMP is a stronger regulator of heat stress-induced repression than activation in both Kc cells and flies.

We next asked whether CLAMP regulates HS-induced gene activation at the genomic level. Therefore, we measured the effect of *clamp* RNAi on transcripts that were activated after HS in control cells (**Figure 1D**, **E**, **Table 1a, c**). We found that 541/995 (54%) of transcripts activated in control *gfp* RNAi cells remain activated after *clamp* RNAi treatment. Furthermore, all well-studied HS-induced transcripts (7), including the *hsp70* gene, are still induced even after *clamp* RNAi treatment (**Table 1d**). Thus, *clamp* RNAi has a more substantial effect on repression (95.6% of repressed genes are no longer repressed) than activation (46% of activated genes are no longer activated). Moreover, the canonical heat stress response *hsp* genes remain activated without CLAMP.

2. CLAMP-associated chromatin loop anchors lost after HS are more frequently near HS-repressed genes than HS-activated genes.

We next asked the question: How does CLAMP regulate transcriptional repression after HS? Repression of transcription after HS is an essential global phenomenon for cells to survive under stress because it conserves energy and prevents the formation of potentially toxic protein and RNA aggregates. CLAMP is known to regulate 3D chromatin loop formation (16), which can be sensitive to changes in temperature (23). Therefore, we asked whether changes in CLAMP-bound 3D loops are associated with HS-induced transcriptional repression.

The function of 3D chromatin organization in the response to HS has remained unclear because the resolution of prior methods was low. One prior report suggests that HS induces the re-localization of architectural proteins from TAD borders to increase long-range interactions enriched with Polycomb marks, thereby regulating repression (12). In plants, HS alters the 3D arrangement of promoter-enhancer interactions to regulate the activation of heat shock-responsive genes (23-25). In contrast, other reports could not find a correlation between global three-dimensional chromatin changes and transcriptional changes after heat shock (2). However, prior studies on 3D chromatin and HS generated HiC data with a resolution of ~40 kb at anchor regions, making it challenging to understand the function of specific chromatin-associated factors, which can be measured at a much higher resolution of approximately 100 bp.

In order to understand precisely how CLAMP functions in transcriptional regulation after HS at high resolution in 3D, we used HiChIP to define CLAMP-associated 3D changes before and after HS. We performed HiChIP using antibodies targeting the CLAMP protein to identify CLAMP-associated loop anchors in cells exposed to HS and matched control NHS cells. Loop anchors bring distal regulatory elements closer to each other, which can regulate activation or repression depending on the factors bound (26,27). Using the FitHiCHIP computational platform (28), we classified CLAMP-associated loop anchors into three classes: 1) loop anchors present in control cells without HS (NHS) (**Fig 2A, N=1515**); 2) loop anchors present after HS (**Fig 2A, N=563**); 3) shared loops anchors that are present in both control (NHS) cells and HS-exposed cells (**Fig 2A**, **N=421**).

Next, we identified CLAMP-associated loop anchors lost and gained during HS. We found CLAMP-associated chromatin loops are lost (**N=980, Fig 2B**) upon HS, and very few are gained

(**N=71, Fig 2B**). Then, we defined the closest gene associated with each loop anchor and examined the overlap between genes associated with loop anchors and genes activated and repressed upon HS. We found a very significant overlap (p-value 2.9778e-60) between genes near CLAMP-associated chromatin loop anchors that are lost upon HS (**N=367/1244, 27.3%**) and genes that are usually repressed by HS (**N=367/1022, 35.9%) (Fig 2C**). Almost all repressed genes (95.6%) are no longer repressed after *clamp* RNAi treatment (**Fig 1E**). Therefore, a significant overlap exists between genes near CLAMP-associated loop anchors lost upon HS (**N=392/1244, 31.5%)** and genes requiring CLAMP for their repression (**Fig 2D, N=392/1034, 37.9%).** Interestingly, a smaller fraction of CLAMP-associated chromatin loops lost after HS (**Fig 2E, N=66/1244; 5%**) also significantly overlap with HS-activated genes (p-value 5.1248e-08). Overall, we identified a more substantial overlap between CLAMP-associated chromatin loop anchors and genes that are repressed than activated by HS.

Then, we categorized CLAMP-associated loop anchors lost after HS (HS Down) and gained after HS (HS Up) into different classes depending on the change in occupancy of CLAMP on chromatin (similar to ChIP-seq) which HiChIP also quantifies in parallel with 3D loop anchors (**Figure S2**): 1) a **H**igh **D**ifference (**HD**) in CLAMP occupancy between HS and NHS conditions; 2) **N**o **D**ifference (**ND**): <25% difference quantified by EdgeR (29,30) in CLAMP occupancy between HS and NHS conditions; 3) **L**ow **D**ifference (LD): >=25% by EdgeR (29,30)in CLAMP occupancy between HS and NHS conditions. Since each loop has two ends, the loop anchors were categorized as HD-HD, HD-LD/ND, ND-ND, LD-ND, and LD-LD loop anchors (**Figure S2A-E**).

We found that most CLAMP-associated loop anchors gained after HS (65/71: 92%) and CLAMP-associated loop anchors lost after HS (849/980: 87%) belong to the ND or LD categories in which CLAMP occupancy on chromatin is not dramatically changed. Furthermore, the ND-ND (3D changes but not 2D changes) class of CLAMP-associated loop anchors lost after HS overlaps significantly with two similar classes of genes: 1) genes repressed after HS in *gfp* RNAi control-treated cells (**Figure S2F**); 2) genes that are de-repressed in *clamp* RNAi cells after HS (**Figure S2G**). Thus, we conclude that upon HS, most CLAMP-associated chromatin changes occur in 3D chromatin contacts between loop anchors rather than in the gain or loss of CLAMP occupancy at

different genomic locations. Furthermore, loss of CLAMP-associated chromatin loop anchor contacts most often occurs at genes that undergo CLAMP-dependent transcriptional repression.

In contrast to CLAMP-associated loop anchors lost after HS, only a small fraction of CLAMP-associated loop anchors gained after HS (N=24/108) overlap with genes that lose repression after *clamp* RNAi (**Figure S3**). Also, CLAMP-associated loop anchors gained upon HS do not significantly overlap with genes activated after HS in normal cells or genes up or down-regulated in *clamp* RNAi cells after HS (**Figure S3**). Therefore, the loss and not the gain of CLAMP-associated loop anchors is most frequently associated with changes in transcriptional repression but not activation upon heat stress.

3. CLAMP-associated chromatin loop anchors are enriched for active chromatin marks prior to heat stress

We next asked the question: What combination of chromatin marks and binding factors distinguish CLAMP-associated loop anchors that will change upon heat stress from other regions of the genome? To address this question, we used available data sets to measure the occupancy of known chromatin marks and binding factors prior to HS at the CLAMP-associated loop anchors that will be lost or gained after HS (**Figure 3**). All CLAMP-bound loop anchors, independent of whether they increase or decrease after HS, were enriched for chromatin marks associated with open chromatin, activation, and enhancers (H4K16ac, H4K20me1, H3K4me3, H3K27ac, H3K4me1)(31-36). Also, all CLAMP-bound loop anchors lacked repressive markers (Su(Hw), CP190, dCTCF, BEAF32, Pc)(26,37).

In contrast, when we measured the occupancy of additional GA-binding TFs, GAF and Psq, at CLAMP-bound loop anchors, we found both these proteins were more enriched at CLAMP-associated loop anchors lost after HS than CLAMP-associated loop anchors gained after HS. CLAMP-associated loop anchors lost after HS were also enriched for the CP-190 interacting insulator binding factors (Ibf1 and Ibf2). However, the CLAMP-associated loop anchors gained

after HS were only enriched for: 1) ZIPIC (Zinc-finger protein interacting with CP190), a promoter-bound TF with architectural and insulator function(38-40), and 2) H3K36me3, a chromatin mark enriched at gene bodies of transcriptionally active genes with roles in co-transcriptional repression and DNA damage repair (35).

Next, we examined the combinatorial relationships between factors bound to CLAMP-associated loop anchors more closely. At enhancer elements, the Psq^S isoform is normally present at 50% of GAF peaks enriched for Polycomb (26). However, CLAMP-associated loop anchors lost after HS, which are enriched for Psq^S, are not enriched for Polycomb (**Figure 3**). Therefore, we identified a subgroup of GAF and Psq^S enriched but Polycomb-depleted CLAMP-associated loop anchors at enhancer elements which lose 3D contacts upon HS. Overall, the combination of GA-binding TFs and other chromatin-associated factors prior to HS differs at CLAMP-associated loop anchors lost compared with those gained after HS.

4. CLAMP-associated loop anchors near HS-repressed and HS-activated genes are associated with different combinations of GA-binding factors prior to HS.

Because we observe significant overlap between CLAMP-associated loop anchors lost after HS and HS-repressed and HS-activated genes (**Figure 2C-E**), we measured the occupancy of chromatin marks and chromatin-bound factors prior to HS at the following classes of loop anchors lost after HS: **Group A**: CLAMP-associated loop anchors lost upon HS which overlap with genes repressed by HS in control *gfp* RNAi cells; **Group B:** CLAMP-associated loop anchors lost upon HS which overlap with genes activated by HS in control *gfp* RNAi treated; **Group C**: CLAMP-associated loop anchors lost upon HS which overlap with genes that are activated in *clamp* RNAi treated cells and therefore require CLAMP for their repression. As shown above, CLAMP occupancy at the loop anchors lost upon HS remains the same before and after HS (**Figure S2**; **Figure 4**). Furthermore, because there is a substantial overlap (N=358) between Group A (genes repressed in *gfp* RNAi control cells, N=367) and Group C (genes that are de-repressed after *clamp* RNAi, N=392), as expected, these groups of genes had similar chromatin marks and binding factors (**Figure 4**).

In contrast, we observed significant differences between chromatin marks and associated factors enriched at CLAMP-associated loop anchors lost after HS, which overlap with genes that will be repressed after HS (**Groups A and C**) and those at genes that will be activated after HS (**Group B**). Genes that will become activated upon HS have higher occupancy of the ZIPIC protein, which recruits the CP190 insulator factor and the Ibf1 and Ibf2 CP190 interacting factors (41). Genes that will become activated upon HS also have increased occupancy of the H3K4me3 active promoter mark and the ISWI chromatin remodeler. However, genes that will become repressed (**Group A and C**) have distinct GAF and Psq^{S} distribution patterns compared to genes that will become activated (**Group B**) (**Figure 4**).

Overall, our data suggest that HS causes CLAMP-bound genes that will become activated (**Group B**) to lose interactions between insulator regions (Figure 2B, Figure 4) bound by ZIPIC, Ibf1, and Ibf2 and CP190. Genes that will become activated are also enriched for ISWI and H3K4me3, which may prime these genes for activation. In contrast, genes that will become repressed are enriched for enhancer marks (**Figure 3**) but also have a distinct localization pattern of PsqS, which is known to recruit the Polycomb group repressor protein and may prime these genes for repression.

Overall, our studies have identified CLAMP as a critical DNA binding factor associated with 3D chromatin loops that drives HS-dependent repression more frequently than HS-dependent activation and suggested a series of combinatorial interactions involved in distinguishing repressed from activated genes. Future work is necessary to define the combinatorial context-specific interactions between all of the factors we identified and other unknown factors that determine whether a gene will become activated or repressed upon heat stress.

Discussion

Temperature is one important abiotic regulator of gene expression that substantially regulates biological functions. Defining how increasing temperature affects gene transcription has not only

identified new transcriptional mechanisms but is vital for managing the effects of global changes in temperature on living organisms including humans, plants, and other animals.

To survive under heat stress, cells must shut down the ongoing transcription of constitutive gene transcripts to avoid accumulating toxic protein products, which would lead to cell death. Compared with decades of work on transcriptional activation upon heat stress (3-5,7), very few reports have provided insight into how HS-induced transcriptional repression is regulated (3,7,10-12,42). In particular, sequence-specific DNA binding factors that target genes for transcriptional repression had yet to be identified.

Here, we demonstrate that the GA-binding transcription factor CLAMP regulates the repression of approximately 95% of repressed genes. In contrast, only a subset of activated genes is regulated by CLAMP, excluding the canonical heat shock response genes encoding heat stress chaperone proteins. Furthermore, we found that CLAMP-associated 3D loop anchors lost upon heat stress are close to repressed genes more often than activated genes, suggesting that local changes in 3D genome organization regulate transcription upon HS. However, the loss of CLAMP-associated loop anchors alone is insufficient to determine whether a gene will be activated or repressed because CLAMP-associated loop anchors are lost upon HS at both repressed and activated genes.

Interestingly, we found that before heat stress, different combinations of GA-binding TFs are enriched at genes that will become activated versus repressed upon HS, suggesting that these combinatorial associations may promote context-specific gene regulation. At CLAMP-associated loop anchors lost but not gained after HS, GAF is co-bound independent of whether a gene will become activated or repressed upon heat stress (**Figure 5**). In contrast, the short isoform of Psq (PsqS) is enriched and bound at a different location at genes that will become repressed upon heat stress compared to genes that will become activated. PsqS has previously been shown to promote enhancer-promoter loop formation and recruit the Polycomb repressor complex (26). However, we identified co-binding of Psq, GAF, and CLAMP at loop anchors lost upon HS that are enriched for active chromatin marks prior to HS (**Group A and C, Figure 4**). We hypothesize that the loss of these loops during HS reduces interactions between enhancer regions and the presence of PsqS

then allows Pc to be recruited, resulting in silencing. Further experiments are required to test this hypothesis.

Another GA-binding protein, GAF, is critical for HS-induced activation but not repression (7). In contrast, CLAMP is more important for repression than activation and CLAMP and GAF can compete for binding or bind synergistically (13). Yet, CLAMP and GAF are both bound at loop anchors lost upon HS that are near both repressed and activated genes. Therefore, the presence of CLAMP versus GAF is not sufficient to determine whether a gene will become activated or repressed. However, we show that a third GA-binding protein, Psq^S, is more enriched at CLAMP-bound loop anchors lost during HS that overlap with HS-repressed genes (**Figure 4**). In contrast, CLAMP-bound loop anchors gained during HS lacked GAF and Psq^S (**Figure 3**). Therefore, our data are consistent with a model in which different combinations of TFs with similar DNA-binding specificities can give rise to differential transcriptional outcomes in a context-specific manner. Mammals also have multiple GA-binding transcription factors, including CTCF and Maz, that may have similar combinatorial context-specific functions but these remain poorly understood (43-45).

In contrast to HS-repressed genes, CLAMP-associated loops lost after HS that overlap with HS-activated genes (**CLASS B, Figure 4**), are enriched for the ZIPIC zinc finger protein prior to HS. ZIPIC is an architectural protein with homodimerization domains that promotes CP190-mediated insulator activity and boundary formation (38-40). Thus, loss of ZIPIC/CP190 enriched CLAMP-associated loops may activate loop-associated genes after HS. Furthermore, we also observed a small but significant overlap between HS-repressed genes and CLAMP-associated loops gained after HS (**Figure S3**). A subset of gained loop anchors are enriched for ZIPIC and, therefore, may be able to recruit CP190 upon HS and promote repression at specific loci. Future work is necessary to define the combinatorial context-specific interactions between all the factors we identified and other unknown factors that determine whether a gene will become activated or repressed upon heat stress.

Also, we have not yet determined how HS results in loss or gain of CLAMP-associated loops. We show that: a) the combination of factors and chromatin marks at CLAMP-associated loop anchors lost and gained upon HS differ from each other; b) CLAMP occupancy on chromatin is not

changed at CLAMP-associated loop anchors that are altered by HS. CLAMP is a intrinsically disordered protein with a prion-like domain PrLD (18). Therefore, we speculate that heat stress may result in biophysical changes at CLAMP-associated loop anchors that regulate the liquid-liquid phase separation properties of bound proteins. Several reports show that increases in temperature influence phase separation properties of disordered proteins with prion-like domains (PrLD) (10,46-50). Hence, it is possible that HS induces changes in the phase separation properties of CLAMP at the loop anchors. The presence of a different combination of chromatin bound factors at different CLAMP-bound target genes may regulate the phase transition properties of the locus which could determine to whether a gene will be activated or repressed upon HS. However, further experiments need to be done to test this hypothesis using *in vitro* chromatin models.

Overall, we show that the GA-binding TF CLAMP is a key DNA binding factor which promotes transcriptional repression after HS versus activation which is important because the mechanism of HS-induced transcriptional repression has remained much less understood that HS-induced activation. We also suggest that different combinations of GA-binding TFs with slightly different DNA binding motifs may prime a gene for activation versus repression upon HS at a particular genomic locus. Overall, we were able to define different combinations of GA-binding factors associated with chromatin loops prior to HS that correlate with gene activation versus repression upon HS. The context-specific combinations of factors we identified provide new insight into how the chromatin landscape at a gene prior to HS may promote rapid activation versus repression upon HS. We also generate new inputs that can be used for developing combinatorial predictive models of how gene expression is rapidly modulated under different conditions.

Material and methods

Fly strains and husbandry

Drosophila melanogaster fly stocks were maintained at 24°C on standard corn flour sucrose media. Fly strains used: *fkh-GAL4* (Bloomington, #78061), *UAS-CLAMPRNAi[val20]* (Bloomington, #57163). These were crossed to obtain the desired genotype, *fkh-GAL4>UAS-CLAMPRNAi*.

Cell culture

Kc cells were maintained at 25°C in Schneider's media supplemented with 10% Fetal Bovine Serum and 1.4X Antibiotic-Antimycotic (Thermofisher Scientific, USA). Cells were passaged every 3 days to maintain an appropriate cell density.

Polytene chromosome squashes and immunostaining after HS

Third instar larvae from undriven *UAS-CLAMPRNAi* and *fkh-GAL4>UAS-CLAMPRNAi* were incubated for 40 min at 37°C in a water bath inside microfuge tube plugged with a soft plug (22) and dissected immediately to pull out the salivary gland. Polytene chromosome squashes were prepared using dissected salivary glands as previously described in Reider et al. 2017(15). We stained polytene chromosomes with rabbit anti-CLAMP (1:1000, SDIX) and mouse anti-RNA pol II (1:500, ab817, Abcam) antibodies. For detection, we used all Alexa Fluor secondary antibodies against rabbit and mouse at a concentration of 1:200 and visualized slides at 40X on a Zeiss Axioimager M1 Epifluorescence upright microscope with the AxioVision version 4.8.2 software.

SLAM-seq

15 ug each of *clamp* dsRNA and GFP dsRNA were used for *clamp* RNAi and GFP RNAi (con), respectively per T25 flask. Kc cells incubated with dsRNA in FBS minus media for 45 minutes and allowed to grow in media supplemented with 10% FBS for 6 days before harvesting. dsRNA targeting *gfp* (control) and *clamp* for RNAi have been previously validated and described (51). PCR products were used as a template to generate dsRNA using the T7 Megascript kit (Ambion, Inc., USA), followed by purification with the Qiagen RNeasy kit (Qiagen, USA).

Two replicates of each for *clamp* RNAi and GFP RNAi, HS (Heat stress) samples and four replicates each for *clamp* RNAi and GFP RNAi, NHS (NHS) samples were used for SLAM-seq. Just before harvesting, cells were either incubated in 4SU (4-thiouridine) provided with SLAMseq Anabolic Kinetics Module (Cat. No. 061.24, Lexogen) at RT or at 37°C for one hour in dark as per manufactures instruction. Cells were immediately harvested and the pellet was resuspended in 1ml of Trizol (Invitrogen, USA). RNA isolated in dark and S4U-labeled transcripts are alkylated with Iodoacteamide as per manufacturer instruction (SLAMseq Explorer and Kinetics Kit user guide, Lexogen). Resulting modified total RNA was used for downstream NGS library preparation

using QuantSeq 3‘mRNA-Seq Library Prep Kit for Illumina (FWD) (Cat. No. 015, Lexogen). Libraries sequenced in Illumina Hiseq 4000 with 150x2 bp pair-end sequencing. For analysis Read 2 for the pair-end sequencing was discarded while performing downstream analysis since quality of Read 2 is very low due to the poly(T) stretch at the beginning of Read 2.

HiChIP

Kc Cells were allowed to grow to confluency and harvested. Before harvesting HS (Heat stress) samples were incubated at 37°C for one hour. 10 x10^6 cells used per HiChIP reaction and two replicates each for NHS (non-heat stress) and HS (Heat stress). Crosslinking performed using 0.3M DSG and 37% formaldehyde as per manufactures protocol (Dovetail™ HiChIP MNase Kit userguide). Dovetail™ HiChIP MNase Kit (Catalog # 21007) that includes the Dovetail Library Prep Kit and the primer set for NGS library preparation was used to digestion, lysate preparation, chromatin immunoprecipitation, proximity ligation and library preparation. Rabbit anti-CLAMP (5µg/sample, SDIX) was used for the immunoprecipitation step. Libraries were subjected to Illumina 150x2 bp pair-end sequencing.

Computational analysis

a) SLAM-seq Analysis

The nf-core/slamseq (v1.0.0) pipeline was used to process and analyze the SLAM-seq data (52,53). The following parameters were used in the pipeline: -profile singularity, --genome BDGP6, --read_length 150, --trim5 12, --polyA 4, --multimappers true, --quantseq false, --endtoend false, --min_coverage 2, --var_fraction 0.2, --conversions 1, --base_quality 27, --pvalue 0.05, --skip_trimming false, --skip_deseq2 false. Adapter trimming was performed using Trim Galore (0.6.5). Conversion-aware mapping, alignment filtering, multimapper recovery, SNP calling, read quantification, gene level quantification collapsing, QC stats, and result summarizations were all performed using SlamDunk (0.4.3)(52). Differentially expressed genes were then determined using DESeq2 (1.22.1).

b) Hi-ChIP Analysis

HiChIP data generated was analyzed using the Dovetail genomics Hi-ChIP documentation (https://hichip.readthedocs.io/en/latest/index.html). Sequences were mapped to the dm6 genome using the Burrows-Wheeler Aligner (0.7.17)(54) passing the following arguments: mem, -5, -S, -P, -T0; default values were used for all other setting. Using the parse module of pairtools (0.3.0), valid ligation events were recorded; the following parameters were changed from default values: --min-mapq 40, --walks-policy 5unique, --max-inter-align-gap 30. PCR duplicates were removed using the dedup module of pairtools (0.3.0). Subsequently, the split module of pairtools was used to generate the final bam and pair files. The samtools (1.17) sort module was used to sort the bam files.

To determine the quality of the proximity ligation events, scripts generated by the Dovetail Genomics team were utilized, which are deposited in the following GitHub repository (https://github.com/dovetail-genomics/HiChiP). The cooler suite (0.9.3)(55) was used to generate contact maps from pair files, and the coolbox API (0.3.9)(56) was used to visualize the contact maps and bigwig tracks. To call loops, the flexible FitHiChIP tool (10.0)(28) was used as resolutions are easily adjustable, and it can detect different categories of 3D chromatin interactions. Furthermore, since FitHiChIP required 1D peaks from the same tissue and conditions, MACS2 (2.2.9.1) was used to call peaks on the Hi-ChIP data. Differential loops between conditions were determined using edgeR in custom scripts located in the FitHiChIP repository (https://github.com/ay-lab/FitHiChIP). Differential loops were visualized as APA plots and loop tracks made with the coolpup.py (57) suite (1.0.0) and coolbox API (0.3.9) (56) respectively.

c) Integration of Hi-ChIP and SLAM-seq datasets

The bedtools suite (2.31.0) was used the extract loop anchors from FitHiChIP output. The overlap statistical analyses between Hi-ChIP loop anchors and SLAM-seq differentially expressed genes were performed using the fisher module of the bedtools suite (2.31.0)(58). The respective overlaps were visualized using the matplotlib-venn (0.11.9) python package.

d) ChIP-seq Analysis

Raw data (GSE118047, GSE30740, GSE36374, GSE36393, GSE54529, GSE63518, GSE80702, GSE89244) was filtered using Trim Galore (0.5.0), then aligned to the dm6 genome using the mem

module of the Burrows-Wheeler Aligner (0.7.17) with default settings. BigWig tracks were produced using the bamCoverage module in the deeptool suite (3.2.1) with the following parameters: --binSize 50, --normalizeUsing CPM, --extendReads 200, --exactScaling, --centerReads, --blackListFileName dm6-blacklist.bed. The respective BigWig tracks were visualized using the coolbox API (0.3.9) and the deeptools suite (3.2.1) over regions of interest.

Competing Interest Statement

The authors declare no conflicting interests.

Acknowledgments

This work and funding to M.R. was supported by R35GM126994 to E.N.L. from NIH. We thank Bloomington stock center for fly lines.

References

1. Richter, K., Haslbeck, M. and Buchner, J. (2010) The heat shock response: life on the verge of death. *Molecular cell*, **40**, 253-266.
2. Ray, J., Munn, P.R., Vihervaara, A., Lewis, J.J., Ozer, A., Danko, C.G. and Lis, J.T. (2019) Chromatin conformation remains stable upon extensive transcriptional changes driven by heat shock. *Proceedings of the National Academy of Sciences*, **116**, 19431-19439.
3. Mahat, D.B., Salamanca, H.H., Duarte, F.M., Danko, C.G. and Lis, J.T. (2016) Mammalian heat shock response and mechanisms underlying its genome-wide transcriptional regulation. *Molecular cell*, **62**, 63-78.
4. Guertin, M., Petesch, S., Zobeck, K., Min, I. and Lis, J. (2010), *Cold Spring Harbor symposia on quantitative biology*. Cold Spring Harbor Laboratory Press, Vol. 75, pp. 1-9.
5. Vihervaara, A., Duarte, F.M. and Lis, J.T. (2018) Molecular mechanisms driving transcriptional stress responses. *Nature Reviews Genetics*, **19**, 385-397.
6. Guertin, M.J. and Lis, J.T. (2010) Chromatin landscape dictates HSF binding to target DNA elements. *PLoS genetics*, **6**, e1001114.
7. Duarte, F.M., Fuda, N.J., Mahat, D.B., Core, L.J., Guertin, M.J. and Lis, J.T. (2016) Transcription factors GAF and HSF act at distinct regulatory steps to modulate stress-induced gene activation. *Genes & development*, **30**, 1731-1746.
8. Wu, C.-H., Yamaguchi, Y., Benjamin, L.R., Horvat-Gordon, M., Washinsky, J., Enerly, E., Larsson, J., Lambertsson, A., Handa, H. and Gilmour, D. (2003) NELF and DSIF cause promoter proximal pausing on the hsp70 promoter in Drosophila. *Genes & development*, **17**, 1402-1414.
9. Li, J., Liu, Y., Rhee, H.S., Ghosh, S.K.B., Bai, L., Pugh, B.F. and Gilmour, D.S. (2013) Kinetic competition between elongation rate and binding of NELF controls promoter-proximal pausing. *Molecular cell*, **50**, 711-722.
10. Rawat, P., Boehning, M., Hummel, B., Aprile-Garcia, F., Pandit, A.S., Eisenhardt, N., Khavaran, A., Niskanen, E., Vos, S.M. and Palvimo, J.J. (2021) Stress-induced nuclear

condensation of NELF drives transcriptional downregulation. *Molecular cell*, **81**, 1013-1026. e1011.

11. Cugusi, S., Mitter, R., Kelly, G.P., Walker, J., Han, Z., Pisano, P., Wierer, M., Stewart, A. and Svejstrup, J.Q. (2022) Heat shock induces premature transcript termination and reconfigures the human transcriptome. *Molecular Cell*, **82**, 1573-1588. e1510.
12. Li, L., Lyu, X., Hou, C., Takenaka, N., Nguyen, H.Q., Ong, C.-T., Cubeñas-Potts, C., Hu, M., Lei, E.P. and Bosco, G. (2015) Widespread rearrangement of 3D chromatin organization underlies polycomb-mediated stress-induced silencing. *Molecular cell*, **58**, 216-231.
13. Kaye, E.G., Booker, M., Kurland, J.V., Conicella, A.E., Fawzi, N.L., Bulyk, M.L., Tolstorukov, M.Y. and Larschan, E. (2018) Differential occupancy of two GA-binding proteins promotes targeting of the drosophila dosage compensation complex to the male X chromosome. *Cell reports*, **22**, 3227-3239.
14. Duan, J., Rieder, L., Colonnetta, M.M., Huang, A., Mckenney, M., Watters, S., Deshpande, G., Jordan, W., Fawzi, N. and Larschan, E. (2021) CLAMP and Zelda function together to promote Drosophila zygotic genome activation. *Elife*, **10**, e69937.
15. Rieder, L.E., Koreski, K.P., Boltz, K.A., Kuzu, G., Urban, J.A., Bowman, S.K., Zeidman, A., Jordan, W.T., Tolstorukov, M.Y. and Marzluff, W.F. (2017) Histone locus regulation by the Drosophila dosage compensation adaptor protein CLAMP. *Genes & development*, **31**, 1494-1508.
16. Jordan, W. and Larschan, E. (2021) The zinc finger protein CLAMP promotes long-range chromatin interactions that mediate dosage compensation of the Drosophila male X-chromosome. *Epigenetics & Chromatin*, **14**, 1-16.
17. Urban, J.A., Urban, J.M., Kuzu, G. and Larschan, E.N. (2017) The Drosophila CLAMP protein associates with diverse proteins on chromatin. *PloS one*, **12**, e0189772.
18. Herzog, V.A., Reichholf, B., Neumann, T., Rescheneder, P., Bhat, P., Burkard, T.R., Wlotzka, W., Von Haeseler, A., Zuber, J. and Ameres, S.L. (2017) Thiol-linked alkylation of RNA to assess expression dynamics. *Nature methods*, **14**, 1198-1204.
19. Soruco, M.M., Chery, J., Bishop, E.P., Siggers, T., Tolstorukov, M.Y., Leydon, A.R., Sugden, A.U., Goebel, K., Feng, J. and Xia, P. (2013) The CLAMP protein links the MSL complex to the X chromosome during Drosophila dosage compensation. *Genes & development*, **27**, 1551-1556.
20. Urban, J., Kuzu, G., Bowman, S., Scruggs, B., Henriques, T., Kingston, R., Adelman, K., Tolstorukov, M. and Larschan, E. (2017) Enhanced chromatin accessibility of the dosage compensated Drosophila male X-chromosome requires the CLAMP zinc finger protein. *PloS one*, **12**, e0186855.
21. Teves, S.S. and Henikoff, S. (2011) Heat shock reduces stalled RNA polymerase II and nucleosome turnover genome-wide. *Genes & development*, **25**, 2387-2397.
22. Lakhotia, S.C., Mallik, M., Singh, A.K. and Ray, M. (2012) The large noncoding hsrω-n transcripts are essential for thermotolerance and remobilization of hnRNPs, HP1 and RNA polymerase II during recovery from heat shock in Drosophila. *Chromosoma*, **121**, 49-70.
23. Huang, Y., An, J., Sircar, S., Bergis, C., Lopes, C.D., He, X., Da Costa, B., Tan, F.-Q., Bazin, J. and Antunez-Sanchez, J. (2023) HSFA1a modulates plant heat stress responses and alters the 3D chromatin organization of enhancer-promoter interactions. *Nature Communications*, **14**, 469.
24. Sun, L., Jing, Y., Liu, X., Li, Q., Xue, Z., Cheng, Z., Wang, D., He, H. and Qian, W. (2020) Heat stress-induced transposon activation correlates with 3D chromatin organization rearrangement in Arabidopsis. *Nature communications*, **11**, 1886.
25. Liang, Z., Zhang, Q., Ji, C., Hu, G., Zhang, P., Wang, Y., Yang, L. and Gu, X. (2021) Reorganization of the 3D chromatin architecture of rice genomes during heat stress. *BMC biology*, **19**, 1-10.

26. Gutierrez-Perez, I., Rowley, M.J., Lyu, X., Valadez-Graham, V., Vallejo, D.M., Ballesta-Illan, E., Lopez-Atalaya, J.P., Kremsky, I., Caparros, E. and Corces, V.G. (2019) Ecdysone-induced 3D chromatin reorganization involves active enhancers bound by Pipsqueak and Polycomb. *Cell reports*, **28**, 2715-2727. e2715.
27. Ogiyama, Y., Schuettengruber, B., Papadopoulos, G.L., Chang, J.-M. and Cavalli, G. (2018) Polycomb-dependent chromatin looping contributes to gene silencing during Drosophila development. *Molecular cell*, **71**, 73-88. e75.
28. Bhattacharyya, S., Chandra, V., Vijayanand, P. and Ay, F. (2019) Identification of significant chromatin contacts from HiChIP data by FitHiChIP. *Nature communications*, **10**, 4221.
29. Robinson, M.D., McCarthy, D.J. and Smyth, G.K. (2010) edgeR: a Bioconductor package for differential expression analysis of digital gene expression data. *bioinformatics*, **26**, 139-140.
30. Chen, Y., Lun, A.T. and Smyth, G.K. (2016) From reads to genes to pathways: differential expression analysis of RNA-Seq experiments using Rsubread and the edgeR quasi-likelihood pipeline. *F1000Research*, **5**.
31. Kyrchanova, O., Sokolov, V. and Georgiev, P. (2023) Mechanisms of Interaction between Enhancers and Promoters in Three Drosophila Model Systems. *International Journal of Molecular Sciences*, **24**, 2855.
32. Cubenas-Potts, C., Rowley, M.J., Lyu, X., Li, G., Lei, E.P. and Corces, V.G. (2017) Different enhancer classes in Drosophila bind distinct architectural proteins and mediate unique chromatin interactions and 3D architecture. *Nucleic acids research*, **45**, 1714-1730.
33. Kyrchanova, O.V., Bylino, O.V. and Georgiev, P.G. (2022) Mechanisms of enhancer-promoter communication and chromosomal architecture in mammals and Drosophila. *Frontiers in Genetics*, **13**, 1081088.
34. Pal, D., Patel, M., Boulet, F., Sundarraj, J., Grant, O.A., Branco, M.R., Basu, S., Santos, S.D., Zabet, N.R. and Scaffidi, P. (2023) H4K16ac activates the transcription of transposable elements and contributes to their cis-regulatory function. *Nature Structural & Molecular Biology*, 1-13.
35. Sharda, A. and Humphrey, T.C. (2022) The role of histone H3K36me3 writers, readers and erasers in maintaining genome stability. *DNA repair*, **119**, 103407.
36. Shoaib, M., Chen, Q., Shi, X., Nair, N., Prasanna, C., Yang, R., Walter, D., Frederiksen, K.S., Einarsson, H. and Svensson, J.P. (2021) Histone H4 lysine 20 mono-methylation directly facilitates chromatin openness and promotes transcription of housekeeping genes. *Nature communications*, **12**, 4800.
37. Kahn, T.G., Savitsky, M., Kuong, C., Jacquier, C., Cavalli, G., Chang, J.-M. and Schwartz, Y.B. (2023) Topological screen identifies hundreds of Cp190-and CTCF-dependent Drosophila chromatin insulator elements. *Science Advances*, **9**, eade0090.
38. Maksimenko, O., Bartkuhn, M., Stakhov, V., Herold, M., Zolotarev, N., Jox, T., Buxa, M.K., Kirsch, R., Bonchuk, A. and Fedotova, A. (2015) Two new insulator proteins, Pita and ZIPIC, target CP190 to chromatin. *Genome research*, **25**, 89-99.
39. Zolotarev, N., Fedotova, A., Kyrchanova, O., Bonchuk, A., Penin, A.A., Lando, A.S., Eliseeva, I.A., Kulakovskiy, I.V., Maksimenko, O. and Georgiev, P. (2016) Architectural proteins Pita, Zw5, and ZIPIC contain homodimerization domain and support specific long-range interactions in Drosophila. *Nucleic acids research*, **44**, 7228-7241.
40. Kaushal, A., Dorier, J., Wang, B., Mohana, G., Taschner, M., Cousin, P., Waridel, P., Iseli, C., Semenova, A. and Restrepo, S. (2022) Essential role of Cp190 in physical and regulatory boundary formation. *Science Advances*, **8**, eabl8834.
41. Cuartero, S., Fresán, U., Reina, O., Planet, E. and Espinàs, M.L. (2014) Ibf1 and I bf2 are novel CP 190-interacting proteins required for insulator function. *The EMBO journal*, **33**, 637-647.

42. Goenka, A., Sengupta, S., Pandey, R., Parihar, R., Mohanta, G.C., Mukerji, M. and Ganesh, S. (2016) Human satellite-III non-coding RNAs modulate heat-shock-induced transcriptional repression. *Journal of cell science*, **129**, 3541-3552.
43. Chetverina, D., Gorbenko, F., Lomaev, D., Georgiev, P. and Erokhin, M. (2022), *Doklady Biochemistry and Biophysics*. Springer, Vol. 506, pp. 210-214.
44. Xiao, T., Li, X. and Felsenfeld, G. (2021) The Myc-associated zinc finger protein (MAZ) works together with CTCF to control cohesin positioning and genome organization. *Proceedings of the National Academy of Sciences*, **118**, e2023127118.
45. Ortabozkoyun, H., Huang, P.-Y., Cho, H., Narendra, V., LeRoy, G., Gonzalez-Buendia, E., Skok, J.A., Tsirigos, A., Mazzoni, E.O. and Reinberg, D. (2022) CRISPR and biochemical screens identify MAZ as a cofactor in CTCF-mediated insulation at Hox clusters. *Nature genetics*, **54**, 202-212.
46. Zhang, H., Shao, S., Zeng, Y., Wang, X., Qin, Y., Ren, Q., Xiang, S., Wang, Y., Xiao, J. and Sun, Y. (2022) Reversible phase separation of HSF1 is required for an acute transcriptional response during heat shock. *Nature cell biology*, **24**, 340-352.
47. Hutin, S., Kumita, J.R., Strotmann, V.I., Dolata, A., Ling, W.L., Louafi, N., Popov, A., Milhiet, P.-E., Blackledge, M. and Nanao, M.H. (2023) Phase separation and molecular ordering of the prion-like domain of the thermosensory protein EARLY FLOWERING 3. *bioRxiv*, 2023.2003. 2012.532276.
48. Dignon, G.L., Zheng, W., Kim, Y.C. and Mittal, J. (2019) Temperature-controlled liquid–liquid phase separation of disordered proteins. *ACS central science*, **5**, 821-830.
49. Chu, W.-T. and Wang, J. (2021) Thermodynamic and sequential characteristics of phase separation and droplet formation for an intrinsically disordered region/protein ensemble. *PLoS computational biology*, **17**, e1008672.
50. Chen, D., Lyu, M., Kou, X., Li, J., Yang, Z., Gao, L., Li, Y., Fan, L.-m., Shi, H. and Zhong, S. (2022) Integration of light and temperature sensing by liquid-liquid phase separation of phytochrome B. *Molecular Cell*, **82**, 3015-3029. e3016.
51. Larschan, E., Soruco, M.M., Lee, O.-K., Peng, S., Bishop, E., Chery, J., Goebel, K., Feng, J., Park, P.J. and Kuroda, M.I. (2012) Identification of chromatin-associated regulators of MSL complex targeting in Drosophila dosage compensation. *PLoS genetics*, **8**, e1002830.
52. Neumann, T., Herzog, V.A., Muhar, M., von Haeseler, A., Zuber, J., Ameres, S.L. and Rescheneder, P. (2019) Quantification of experimentally induced nucleotide conversions in high-throughput sequencing datasets. *BMC bioinformatics*, **20**, 1-16.
53. Ewels, P.A., Peltzer, A., Fillinger, S., Patel, H., Alneberg, J., Wilm, A., Garcia, M.U., Di Tommaso, P. and Nahnsen, S. (2020) The nf-core framework for community-curated bioinformatics pipelines. *Nature biotechnology*, **38**, 276-278.
54. Li, H. and Durbin, R. (2009) Fast and accurate short read alignment with Burrows–Wheeler transform. *bioinformatics*, **25**, 1754-1760.
55. Abdennur, N. and Mirny, L.A. (2020) Cooler: scalable storage for Hi-C data and other genomically labeled arrays. *Bioinformatics*, **36**, 311-316.
56. Xu, W., Zhong, Q., Lin, D., Zuo, Y., Dai, J., Li, G. and Cao, G. (2021) CoolBox: a flexible toolkit for visual analysis of genomics data. *BMC bioinformatics*, **22**, 1-9.
57. Flyamer, I.M., Illingworth, R.S. and Bickmore, W.A. (2020) Coolpup. py: versatile pile-up analysis of Hi-C data. *Bioinformatics*, **36**, 2980-2985.
58. Quinlan, A.R. and Hall, I.M. (2010) BEDTools: a flexible suite of utilities for comparing genomic features. *Bioinformatics*, **26**, 841-842.

Figure legend

Figure 1. CLAMP regulates heat-stressed induced transcriptional repression more strongly than activation

A. Scatter plot showing significant changes (log2FC ≥2 and p≥0.05) in the levels of nascent transcripts (red dots) present after HS (heat stress) compared to the control NHS (No heat stress) condition in control (*gfp* RNAi) cells.

B. Scatter plot showing significant changes (log2FC ≥2 and p≥0.05) in the levels of nascent transcripts (red dots) transcribed after HS (heat stress) in the absence of CLAMP (*clamp* RNAi) compared to control (*gfp* RNAi) cells. Dotted horizontal lines in **A** and **B** denote ± 2 $\log_2$FC change cutoffs.

C. Immunofluorescence, images of HS (37^0C for 1 Hr) salivary gland polytene, spreads showing the distribution of active RNA polymerase II (red) on chromatin (blue) in the presence (undriven *clamp RNAi*) and absence (*fkh-GAL4>clampRNAi*) of CLAMP (green). Scale bar (100uM) applies to both panels in **C**.

D-E. Venn diagrams comparing HS-activated transcripts (Maroon circle in **D**) and HS-repressed transcripts (Green circle in **E**) from control cells (*gfp* RNAi*)* to HS-activated (red circle) and HS-repressed (olive circle) transcripts in *clamp* RNAi treated cells.

Figure 2. CLAMP-bound loop anchors lost during heat stress overlap more significantly with CLAMP-dependent repressed genes than CLAMP-dependent activated genes

A. 2D metaplot of CLAMP HiChIP loop anchors centered on three classes of significant loop anchor interactions identified by CLAMP HiChIP in both NHS and HS conditions: 1) Loop anchors identified only in NHS conditions (control loop anchors, N=1515); 2) Loop anchors identified in **both** NHS and HS conditions (shared Loop anchors, N=421) and 3) Loop anchors identified only in HS conditions (HS loop anchors, N=563). The value listed indicates the enrichment of the center pixel compared with the top left corner.

B. 2D metaplot of CLAMP HiChIP data centered on significant interactions identified from CLAMP HiChIP under NHS or HS conditions for **differential** loop anchors gained after HS (HS

Up loop anchors, N=71) or loop anchors lost after HS (HS Down loop anchors, N=980). The score indicates the enrichment of the center pixel compared with the top left corner.

C. Venn diagram showing significant overlap between CLAMP-associated loop anchors lost during HS (N=1244) with genes normally repressed (N=1022) after HS (Fisher test, p=2.9778e-60).

D. Venn diagram showing significant overlap between CLAMP-associated loop anchors lost during HS (N=1244) with genes activated (N=1034) after HS in cells treated with *clamp* RNAi. (Fisher test, p=2.8996e-66).

E. Venn diagram showing the significant overlap between CLAMP-associated loop anchors lost during HS (N=1244) with genes usually activated (N=420) after HS in *gfp* control RNAi treated cells (Fisher test, p=5.1248e-08).

Figure 3. CLAMP-bound HS lost and gained loop anchors have different chromatin-bound factors prior to heat stress

Average enrichment of different class of chromatin bound factors mentioned at the top of each panel and corresponding heatmap centered around ±1kb of CLAMP-associated HS lost loop anchors (blue line) and CLAMP-associated HS gained loop anchors (green line). Lines indicate mean enrichment, with shaded areas representing standard deviation.

Figure 4. HS repressed and activated genes have a differential distribution of GAF, Psq^{S}, ISWI, Ibf, and ZIPIC

Average enrichment of different chromatin bound factors is labeled at the top of each panel and the corresponding heatmap centered around ±1kb of CLAMP-associated HS lost loop anchors which overlap with: **CLASS A** (genes repressed by HS in control (Navy blue line)), **CLASS B** (genes activated by HS in control (Turquoise blue line) and **CLASS C** (genes that are activated in *clamp* RNAi treated cells (Yellow line)). Lines indicate mean enrichment, with shaded areas representing standard deviation.

Figure 5. Differential combination of GA-binding zinc finger proteins bound to CLAMP-associated loop anchors prior to HS are associated with different transcriptional outputs upon HS. Schematic shows hypothetical model predicting how combinations of different C2H2 zinc finger DNA binding proteins that bind prior to HS may regulate transcriptional changes induced during heat stress.

Supplementary figure legend

Fig. S1 CLAMP functions more frequently as a repressor than an activator in both NHS and HS conditions.

A-B. Scatter plots showing more up-regulated nascent transcripts (positive red dots, $p \geq 0.05$, log2FC ≥ 2) both under NHS (No heat stress) and HS (heat stress) conditions in *clamp* RNAi-treated cells.

Fig S2. Most CLAMP-associated changes upon heat stress are three-dimensional and not associated with differences in CLAMP occupancy.

A-E. Example tracks for each class of CLAMP-associated loops lost and gained after HS. The grey tracks show the occupancy of CLAMP after HS, whereas the purple tracks show CLAMP occupancy in normal conditions (NHS). A purple line connects loop anchor endpoints. The classes of CLAMP-associated loops shown are **A**) HD-HD, in which there is a change in both three-dimensional contacts and CLAMP occupancy at both ends of the loop anchor after HS; **B**) HD-ND, in which there is a change in 3D contacts and occupancy of CLAMP at one end of the loop anchor after HS; **C**) ND-ND, in which there is only a change in 3D contacts and no change in CLAMP occupancy at either end of the loop anchor after HS; **D**) ND-LD in which there is a change in 3D contacts and only a slight change in CLAMP occupancy at one of the ends of the loop anchor after HS; **E**) LD-LD in which there is a change in 3D contacts and only a slight change in CLAMP occupancy at both of the ends of the loop anchor after HS.

F. Venn diagram comparing CLAMP-associated loop anchors lost during HS (N=931) without any difference in CLAMP occupancy after HS (ND-ND class) with genes normally repressed (N=1022) after HS (Fisher's exact test, p <1.9471e-23).

G. Venn diagram comparing CLAMP-associated loop anchors lost during HS (N=931) without any difference in CLAMP occupancy after HS (ND-ND class) with genes activated (N=1034) after HS in cells treated with *clamp* RNAi. (Fisher's exact test, p<2.07556e-24).

H. Venn diagram comparing CLAMP-associated loop anchors lost during HS (N=931) without any difference in CLAMP occupancy after HS (ND-ND class) with genes usually activated (N=420) after HS in *gfp* RNAi treated cells (Fisher's exact test, p <0.09047).

Fig S3. A small fraction of CLAMP-bound loop anchors gained during heat stress overlap with CLAMP-dependent repressed genes.

A-B. Venn diagram showing the overlap between CLAMP-associated loop anchors gained during HS (N=108) and genes normally repressed (N=1022) after HS after control *gfp* RNAi treatment (**A**) (Fisher test, p=0.00838) and with genes usually activated (N=420) after HS (**B**) (Fisher test, p=0.2056)

C-D. Venn diagram showing the overlap between CLAMP-associated loop anchors gained during HS (N=108) with genes repressed (N=30) after HS in cells treated with *clamp*RNAi (**C**) (Fisher test, p=1) and with genes activated (N=1034) after HS in cells treated with *clamp*RNAi (**D**) (Fisher test, p=0.010796).

Table legend

Table 1a. List of differentially transcribed RNA transcripts after heat stress (HS) compared to non-heat stress condition (NHS) in control (*gfp RNAi*)

Table 1b. List of differentially transcribed RNA transcripts under non-heat stress condition (NHS) in *Clamp RNAi* compared to control *gfp RNAi*

Table 1c. List of differentially transcribed RNA transcripts after heat stress (HS) compared to non-heat stress condition (NHS) in *Clamp RNAi*

A

HS vs NHS in Control (*gfpRNAi*)

N=17600

Up-regulated transcripts=995

Activated gene transcripts

Down-regulated transcripts=3547

Repressed gene transcripts

log2FC

Average Expression total mRNA (RPM)

B

clampRNAi vs *gfpRNAi* in HS

N=15851

Up-regulated transcripts=4028

Activated gene transcripts

Down-regulated transcripts=58

Repressed gene transcripts

log2FC

Average Expression total mRNA (RPM)

C

undriven *CLAMPRNAi*

fkh-GAL4>CLAMPRNAi

HS

100 µm

CLAMP+ RNApol II + DAPI

D

N=1192
HS Activated in *ClampRNAi*

N=995
HS Activated in *gfpRNAi*

N=194
HS Repressed in *ClampRNAi*

651

541

454

194

E

N=3547
HS Repressed in *gfpRNAi*

N=1192
HS Activated in *ClampRNAi*

N=194
HS Repressed in *ClampRNAi*

1046

146

3246

155

39

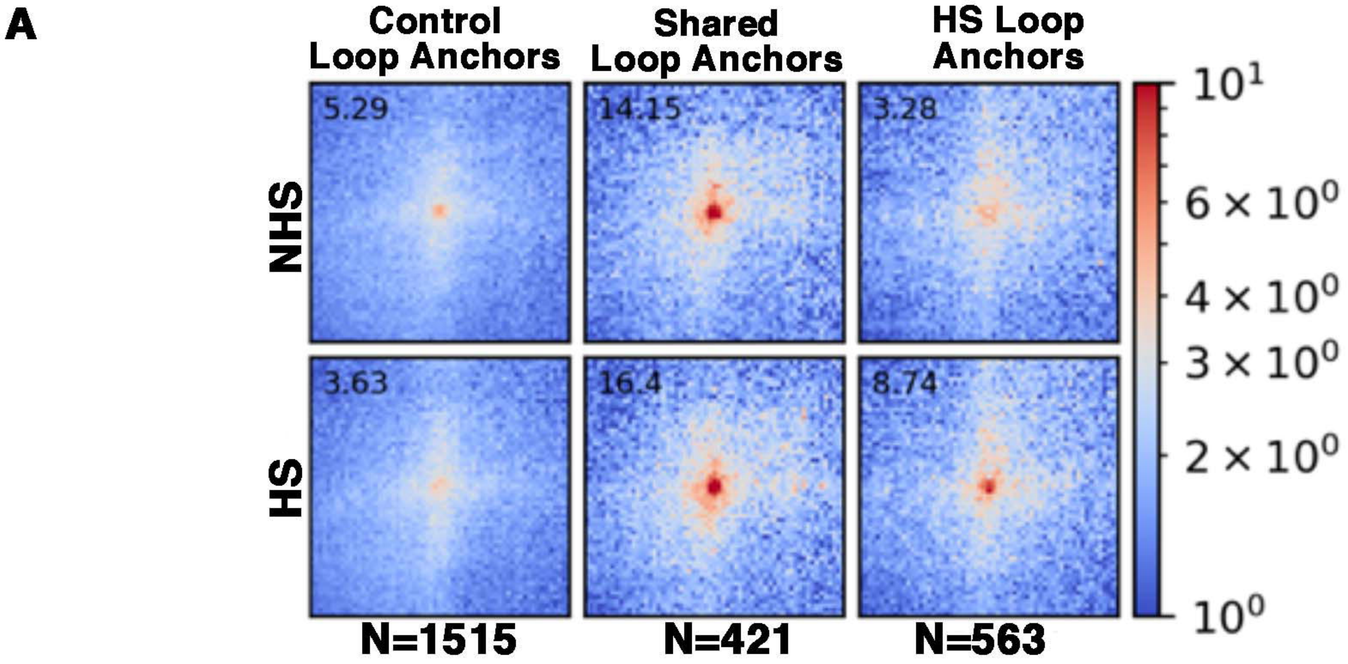

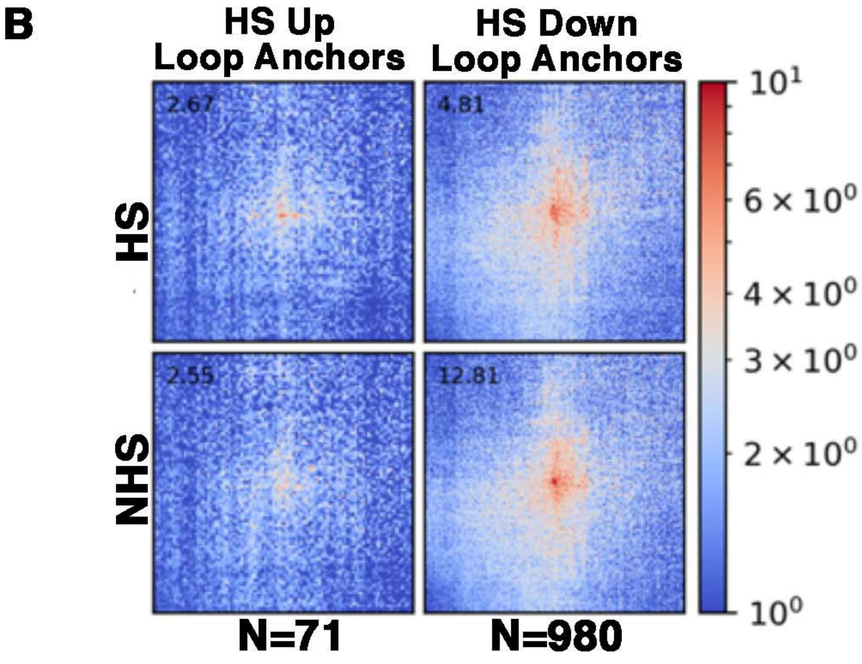

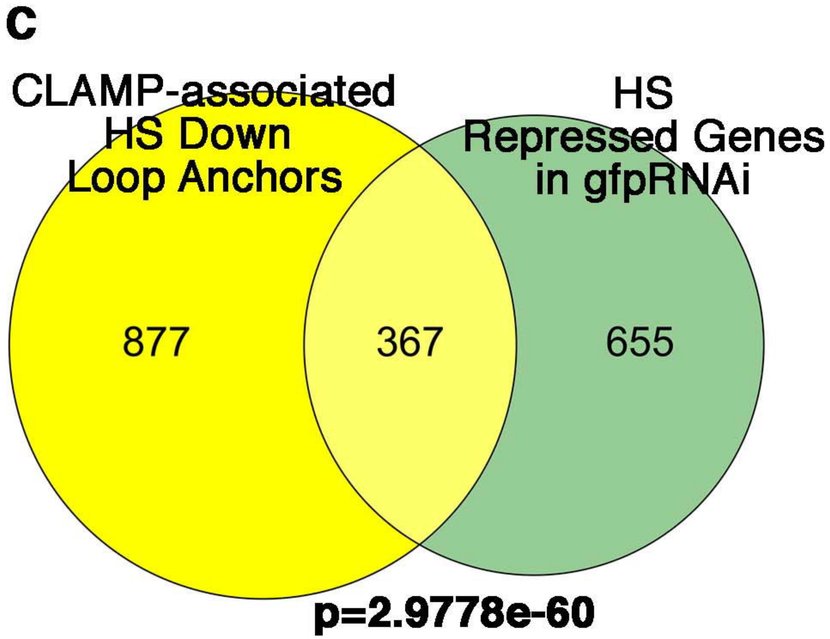

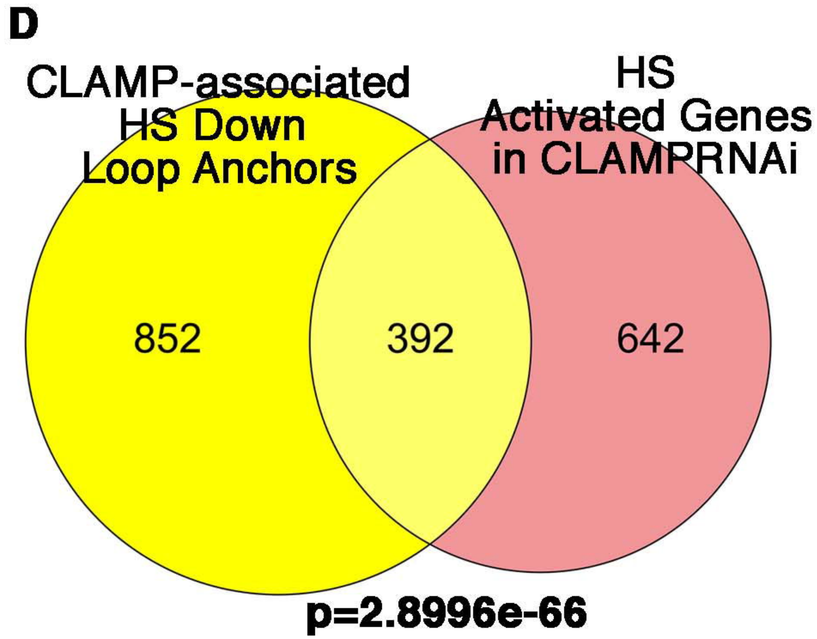

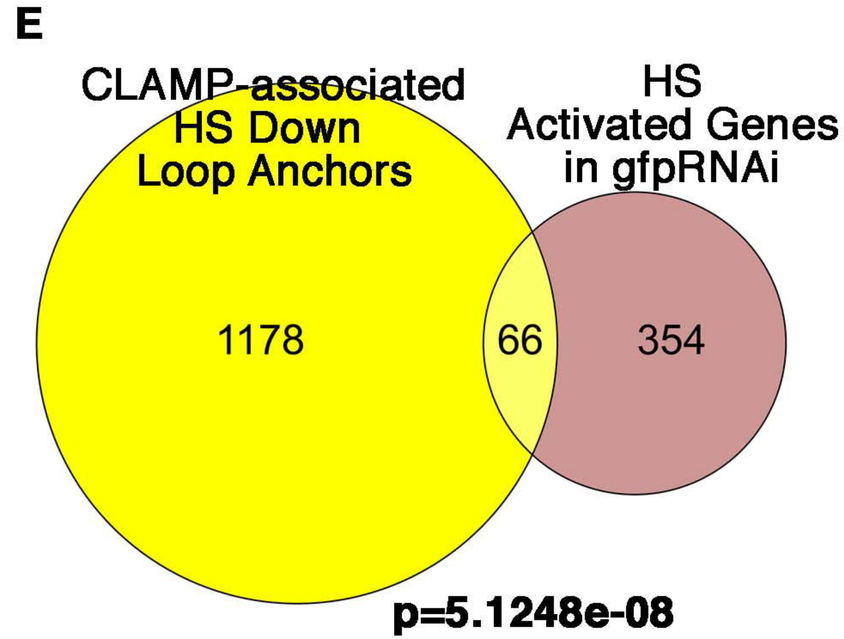

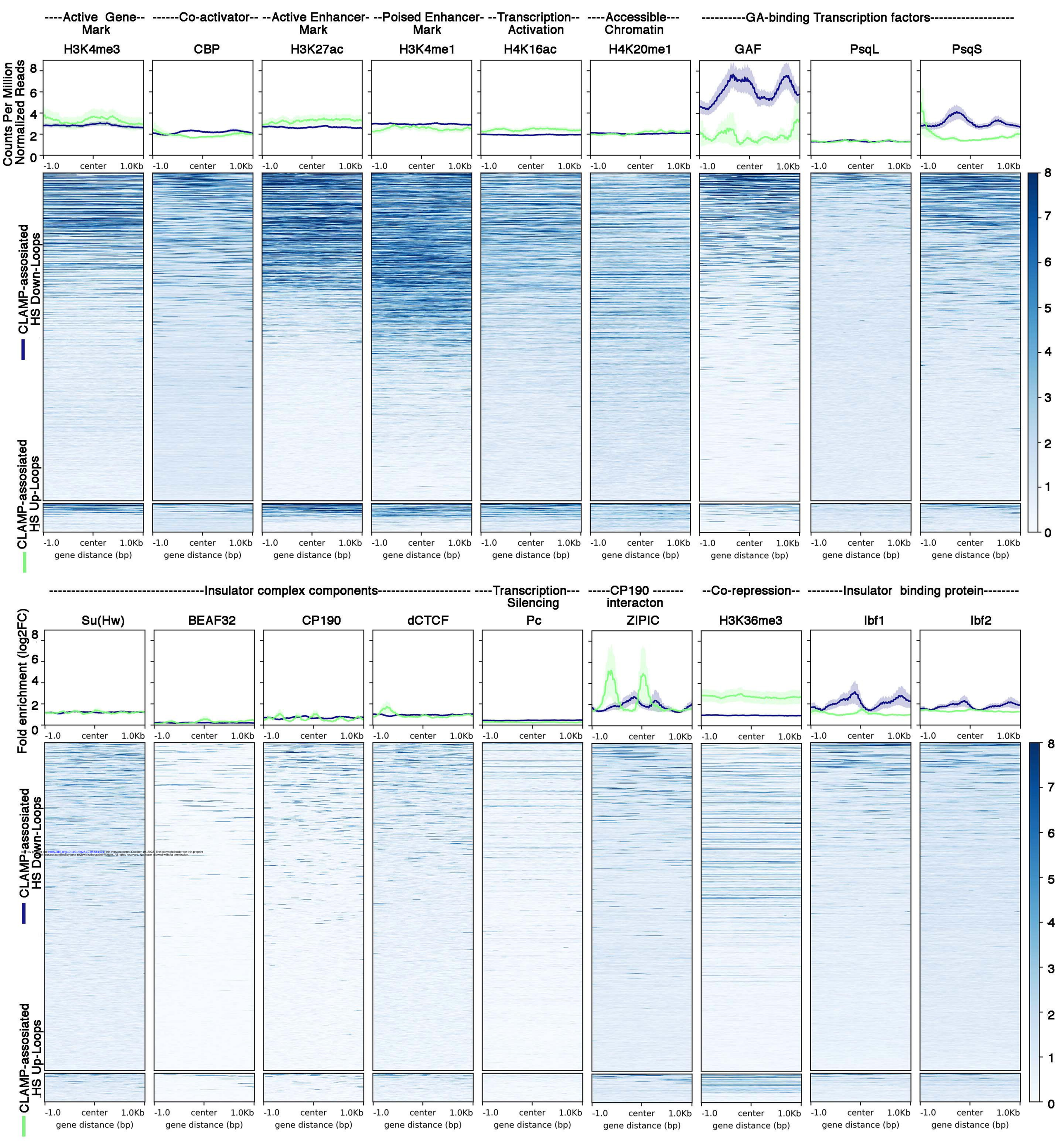

CLAMP(NHS)
CLAMP(HS)
ISWI
PsqL
PsqTot
CLASS A
CLASS B
CLASS C
-1.0
center
1.0Kb
gene distance (bp)
CP190
GAF
Ibf1
Ibf2
ZIPIC
H3K4me3

Enhancer marks

GAF

CLAMP

Psq

Chromatin Loops Lost

Enhancer marks

Polycomb

HS-Repression

CP190

ZIPIC

Chromatin Loops Lost

CP190

HS-Activation

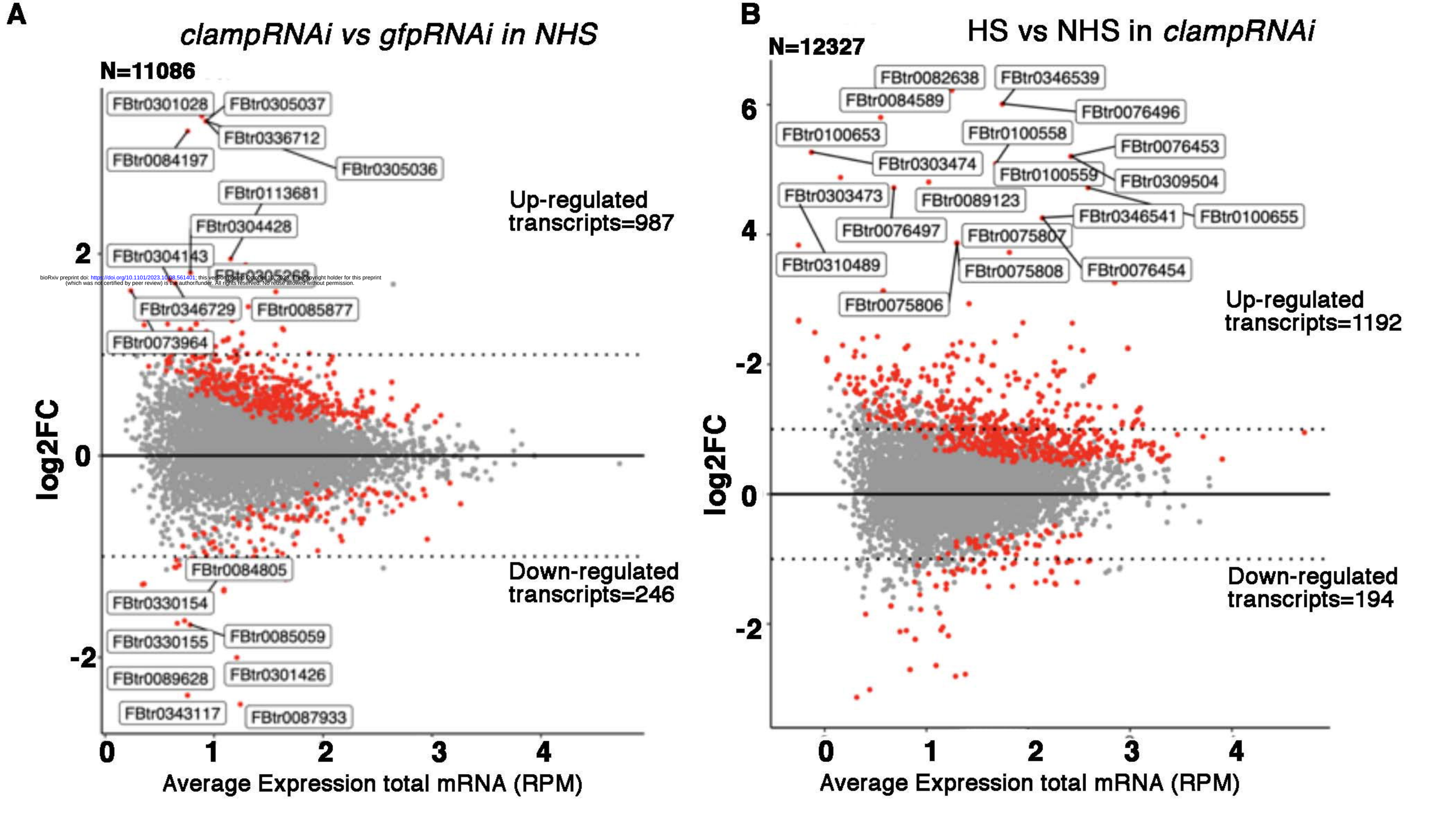

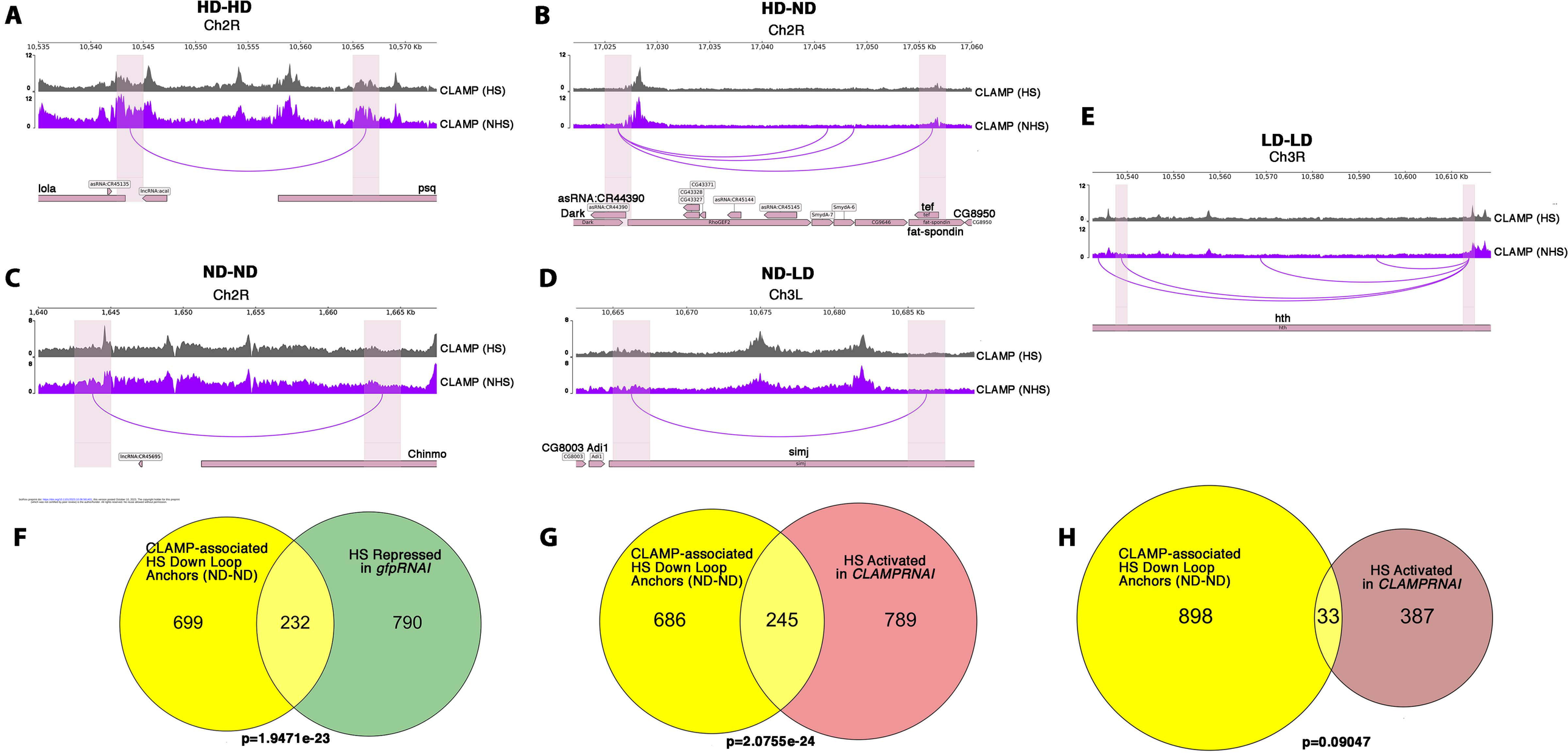
A
HD-HD
Ch2R
10,535
10,540
10,545
10,550
10,555
10,560
10,565
10,570 Kb
CLAMP (HS)
CLAMP (NHS)
lola
asRNA:CR45135
lncRNA:acal
psq
B
HD-ND
Ch2R
17,025
17,030
17,035
17,040
17,045
17,050
17,055 Kb
17,060
CLAMP (HS)
CLAMP (NHS)
asRNA:CR44390
Dark
CG43371
CG43328
CG43327
asRNA:CR45144
asRNA:CR45145
SmydA-7
SmydA-6
tef
CG8950
fat-spondin
RhoGEF2
CG9646
C
ND-ND
Ch2R
1,640
1,645
1,650
1,655
1,660
1,665 Kb
CLAMP (HS)
CLAMP (NHS)
lncRNA:CR45695
Chinmo
D
ND-LD
Ch3L
10,665
10,670
10,675
10,680
10,685 Kb
CLAMP (HS)
CLAMP (NHS)
CG8003
Adi1
simj
E
LD-LD
Ch3R
10,540
10,550
10,560
10,570
10,580
10,590
10,600
10,610 Kb
CLAMP (HS)
CLAMP (NHS)
hth
F
CLAMP-associated HS Down Loop Anchors (ND-ND)
699
232
HS Repressed in gfpRNAI
790
p=1.9471e-23
G
CLAMP-associated HS Down Loop Anchors (ND-ND)
686
245
HS Activated in CLAMPRNAI
789
p=2.0755e-24
H
CLAMP-associated HS Down Loop Anchors (ND-ND)
898
33
HS Activated in CLAMPRNAI
387
p=0.09047

A

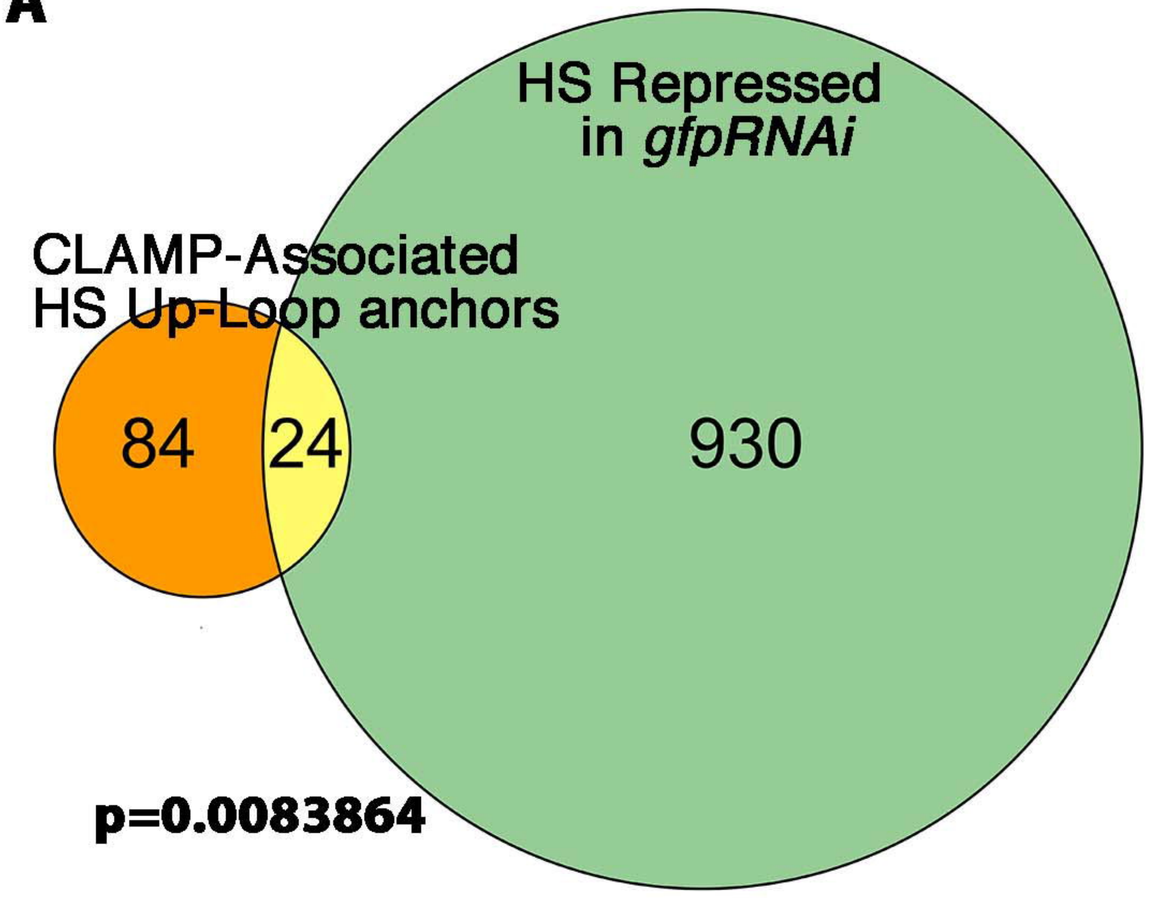

B

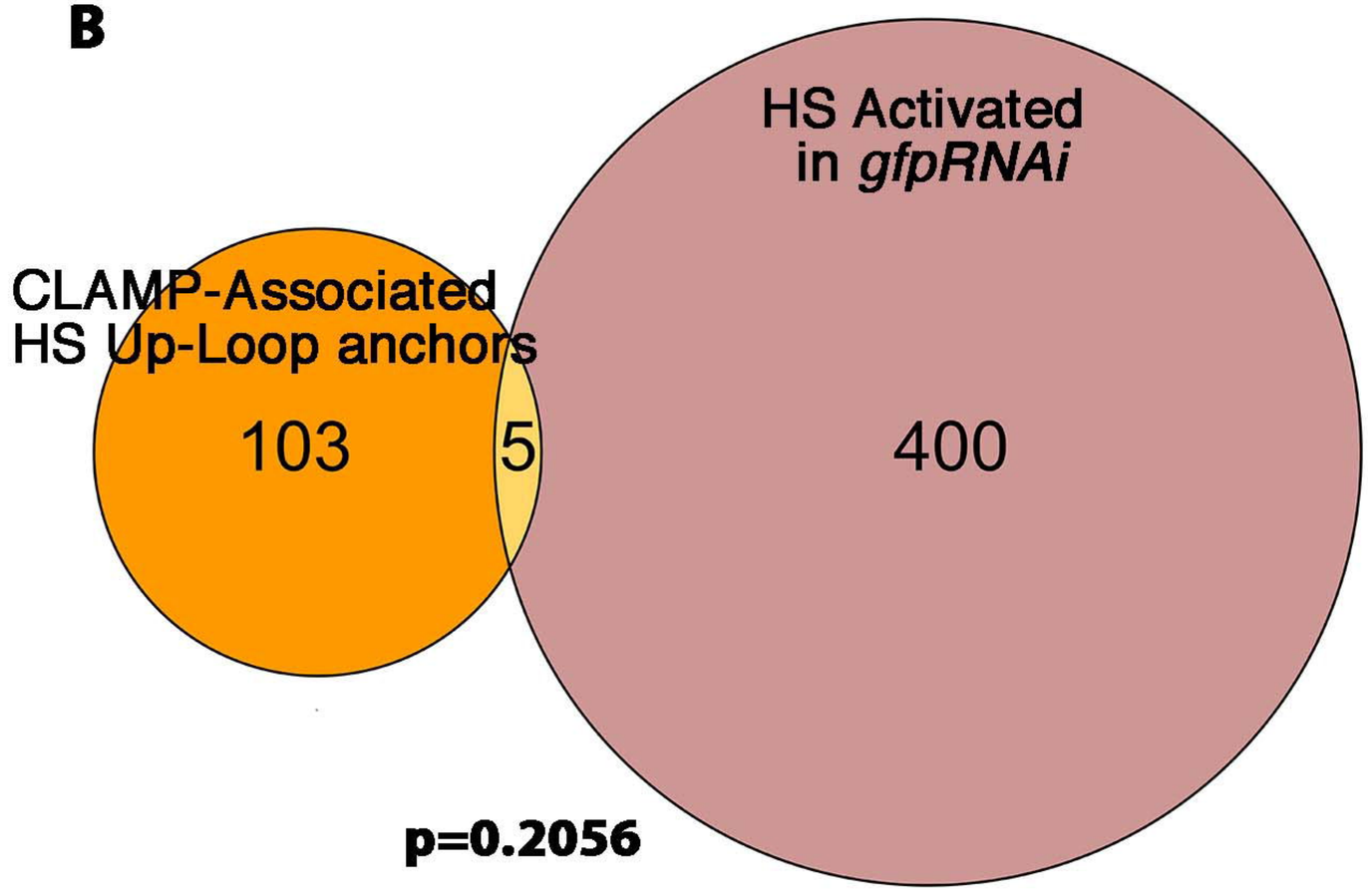

C

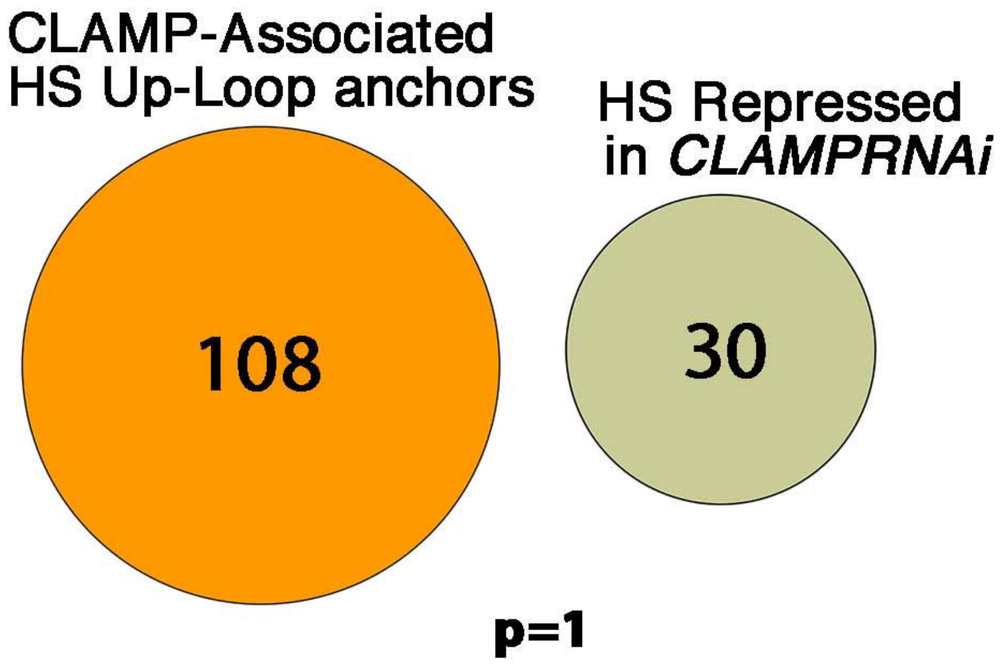

D